Catalytic Activity of Bis-phosphine Ruthenium(II)−Arene Compounds: Structure−Activity Correlations

Adrian B. Chaplin and Paul J. Dyson*

Institut des Sciences et Ingénierie Chimiques, Ecole Polytechnique Fédérale de Lausanne (EPFL), CH-1015 Lausanne, Switzerland

Received January 18, 2007

The phosphine dissociation characteristics of a range of bis-phosphine ruthenium(II)−arene complexes, $[Ru(PPh_3)(PR_3)(\eta^6\text{-arene})]PF_6$ (arene = *p*-cymene: PR_3 = $PPhMe_2$, PPh_3, P(*p*-tol)$_3$, $PPh_2{}^iPr$; arene = PhMe: PR_3 = $PPhMe_2$, PPh_3), $[Ru(PPh_3)(\eta^2\text{-}PPh_2(C_6H_4O))(\eta^6\text{-}p\text{-cymene})]PF_6$, and $[RuCl(PPh_3)(\eta^7\text{-}PPh_2(CH_2)_3Ph)]PF_6$, have been investigated by a combination of ligand exchange kinetics (with P(*p*-tol)$_3$ in THF) and tandem electrospray ionization mass spectrometry (ESI-MS/MS). Trends in reactivity established from these studies were rationalized in terms of steric bulk, on the arene or phosphine, and conformational freedom of the phosphine ligands. A good correlation is found between these trends, especially from the ESI-MS/MS data, and activity of the complexes as catalyst precursors for the hydrogenation of styrene to ethyl benzene (in THF). The most active catalyst precursors show good activity under comparatively mild conditions (e.g., TOF ≥ 2000 h^{-1} for styrene hydrogenation in THF at 50 °C under 50 bar of H_2). The X-ray structures of $[RuCl(PPh_3)(PPhMe_2)(\eta^6\text{-}p\text{-cymene})]PF_6$, $[RuCl(PPh_3)(PPh_2{}^iPr)(\eta^6\text{-}p\text{-cymene})]PF_6$, $[RuCl(PPh_3)(P(p\text{-tol})_3)(\eta^6\text{-}p\text{-cymene})]PF_6$, and $[RuCl(\eta^2\text{-}PPh_2(C_6H_4O))(\eta^6\text{-}p\text{-cymene})]$ are also reported.

Introduction

Half-sandwich ruthenium(II)−arene complexes are an important and widely used class of organometallic compound, which exhibit a diverse range of coordination chemistry and show considerable potential as precursors for catalytic organic transformations.[1,2] Among these complexes, those bearing one η^1-phosphine ligand have been established as useful catalyst precursors for a wide range of reactions. Examples include hydrogenation,[3] free-radical polymerization of vinyl monomers,[4] dienylalkyne cyclization,[5] olefin cyclopropanation,[6] the *anti*-Markovnikov hydration of terminal alkynes,[7] and the propargylation of heterocycles with propargyl alcohols.[8] Furthermore, cationic allenylidene complexes bearing phosphine co-ligands, e.g., $[Ru(=C=C=CPh_2)Cl(PR_3)(\eta^6\text{-}p\text{-cymene})]^+$, have found applications as catalysts for olefin metathesis.[9]

Given that a large number of molecular catalysts require a ligand dissociation step (typically dissociation of phosphine) in order for the catalysts to enter the catalytic cycle,[10] we decided to investigate the reactivity of a variety of bis-phosphine ruthenium(II)−arene complexes, comprising triphenylphosphine

Chart 1[a]

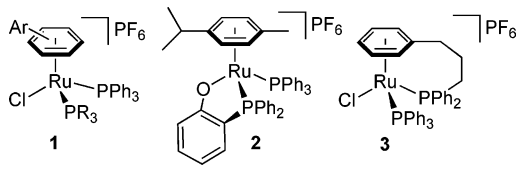

[a] Arene = *p*-cymene: PR_3 = $PPhMe_2$ (**1a**), PPh_3 (**1b**), P(*p*-tol)$_3$ (**1c**), $PPh_2{}^iPr$ (**1d**). Arene = PhMe: PR_3 = $PPhMe_2$ (**1e**), PPh_3 (**1f**).

Scheme 1

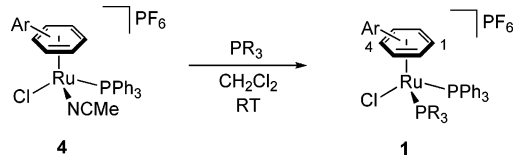

* E-mail: paul.dyson@epfl.ch.

(1) For examples see: (a) Rigby, J. H.; Kondratenko, M. A. *Top. Organomet. Chem.* **2004**, *7*, 181. (b) Geldbach, T. J.; Dyson, P. J. *J. Am. Chem. Soc.* **2004**, *126*, 8114. (c) Naota, T.; Takaya, H.; Murahashi, S.-I. *Chem. Rev.* **1998**, *98*, 2599. (d) Noyori, R.; Hashiguchi, S. *Acc. Chem. Res.* **1997**, *30*, 97. (e) Bennett, M. A. *Coord. Chem. Rev.* **1997**, *166*, 225. (f) Bennett, M. A In *Comprehensive Organometallic Chemistry II*; Abel, E. W., Stone, F. G. A., Wilkinson, G., Eds.; Elsevier: Oxford, 1995; Vol. 7, p 549. (g) Le Bozec, H.; Touchard, D.; Dixneuf, P. H. *Adv. Organomet. Chem.* **1989**, *29*, 163.

(2) For examples see: (a) Qiu, L.; Kwong, Y.; Wu, J.; Lam, W. H.; Chan, S.; Yu, W.-Y.; Li, Y.-M.; Guo, R.; Zhou, Z.; Chan, A. S. C. *J. Am. Chem. Soc.* **2006**, *128*, 5955. (b) Daguenet, C.; Dyson, P. J. *Organometallics* **2006**, *25*, 5811. (c) Daguenet, C.; Scopelliti, R.; Dyson, P. J. *Organometallics* **2004**, *23*, 4849. (d) Daguenet, C.; Dyson, P. J. *Organomatallics* **2004**, *23*, 6080. (e) Ghebreyessus, K. Y.; Nelson, J. H. *J. Organomet. Chem.* **2003**, *669*, 48. (f) Mashima, K.; Kusano, K.-H.; Sato, N.; Matsumura, Y.-I.; Nozaki, K.; Kumobayashi, H.; Sayo, N.; Hori, Y.; Ishizaki, T.; Akutagawa, S.; Takaya, H. *J. Org. Chem.* **1994**, *59*, 3064.

(3) (a) Geldbach, T. J.; Laurenczy, G.; Scopelliti, R.; Dyson, P. J. *Organometallics* **2006**, *25*, 733. (b) Bennett, M. A.; Huang, T. -N.; Smith, A. K.; Turney, T. W. *J. Chem. Soc., Chem. Commun.* **1978**, 583.

(4) Simal, F.; Demonceau, A.; Noels, A. F. *Angew. Chem., Int. Ed.* **1999**, *38*, 538.

(5) Merlic, C. A.; Pauly, M. E. *J. Am. Chem. Soc.* **1996**, *118*, 11319.

(6) (a) Leadbeater, N. E.; Scott, K. A.; Scott, L. J. *J. Org. Chem.* **2000**, *65*, 3231. (b) Simal, F.; Jan, D.; Demonceau, A.; Noels, A. F. *Tetrahedron Lett.* **1999**, *40*, 1653.

(7) (a) Hansen, H. D.; Nelson, J. H. *Organometallics* **2000**, *19*, 4740. (b) Tokunaga, M.; Wakatsuki, Y. *Angew. Chem., Int. Ed.* **1998**, *37*, 2867.

(8) Bustelo, E.; Dixneuf, P. H. *Adv. Synth. Catal.* **2005**, *347*, 393.

(9) (a) Castarlenas, R.; Dixneuf, P. H. *Angew. Chem., Int. Ed.* **2003**, *42*, 4524. (b) Bassetti, M.; Centola, F.; Sémeril, D.; Bruneau, C.; Dixneuf, P. H. *Organometallics* **2003**, *22*, 4459. (c) Akiyama, R.; Kobayashi, S. *Angew. Chem., Int. Ed.* **2002**, *41*, 2602. (d) Fürstner, A.; Liebl, M.; Lehmann, C. W.; Picquet, M.; Kunz, R.; Bruneau, C.; Touchard, D.; Dixneuf, P. H. *Chem.−Eur. J.* **2000**, *6*, 1847. (e) Picquet, M.; Bruneau, C.; Dixneuf, P. H. *Chem. Commun.* **1998**, 2249. (f) Fürstner, A.; Picquet, M.; Bruneau, C.; Dixneuf, P. H. *Chem. Commun.* **1998**, 1315.

(10) Cotton, F. A.; Wilkinson, G.; Murillo, C. A.; Bochman, M. *Advanced Inorganic Chemistry*, 6th ed.; John Wiley & Sons: New York, 1999.

10.1021/om070050d CCC: $37.00
Publication on Web 03/23/2007

Scheme 2

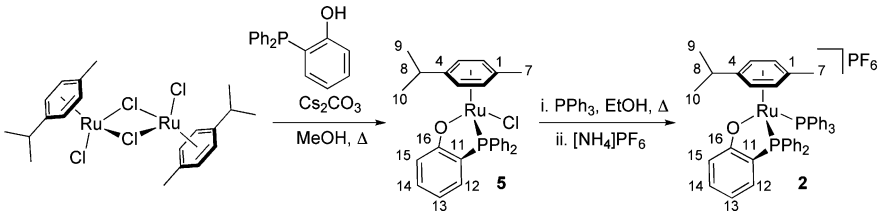

Table 1. Selected $^{31}P\{^1H\}$ and $^{13}C\{^1H\}$ NMR Data for $[RuCl(PPh_3)(PR_3)(\eta^6\text{-arene})]PF_6$ ($CDCl_3$, 293 K)[a]

	1a	**1b**	**1c**	**1d**	**1e**	**1f**	**2**	**3**[b]
arene			*p*-cymene			PhMe	*p*-cymene	
PR_3	$PPhMe_2$	PPh_3	$P(p\text{-tol})_3$	$PPh_2{}^iPr$	$PPhMe_2$	PPh_3	$PPh_2(C_6H_4O)$	$PPh_2(CH_2)_3Ph$
PPh_3	27.0	20.8	20.3	23.5	31.9	22.4	26.0	22.9
PR_3	3.5		19.8	18.8	3.7		54.3	17.5
$^2J_{PP}$	54		52	50	56		48	51
C^1	99.0	100.7	100	98.8	84.0	83.5	99.0	96.3
C^4	128.0	131.8	134	132	118.0	122.6	123.1	101.0

[a] Labels as in Schemes 1 and 2. Chemical shifts in ppm and coupling constants (J) in Hz. [b] From ref 12, in $(CD_3)_2CO$; assignment of $^{31}P\{^1H\}$ NMR data has been corrected. $C^1 = i\text{-}C_6H_4(CH_2)_3PPh_2$ and $C^4 = p\text{-}C_6H_4(CH_2)_3PPh_2$.

and other η^1-phosphines of varying electronic strength and steric bulk, of general formula $[RuCl(PPh_3)(PR_3)(\eta^6\text{-arene})]PF_6$ (**1**), an anionic bidentate *ortho*-oxy-substituted phosphine (**2**), and an arene-tethered phosphine (**3**), Chart 1. Although a number of complexes of this type have previously been reported,[1f,g] there is a paucity of investigations into their catalytic activity and dissociation characteristics. This is somewhat surprising given the utility of the monophosphine complexes and the related diphosphine complexes.[2] Seeking to explore the catalytic value of this class of complex, we report here an investigation of their phosphine dissociation characteristics and activity as catalyst precursors for the hydrogenation of styrene. A combination of tandem electrospray ionization mass spectrometry (ESI-MS/MS) and ligand exchange kinetics has been used to assess their dissociation properties, and correlations with their catalytic activity are highlighted.

Results and Discussion

1. Synthesis. The preparation of the bis-phosphine complexes $[Ru(PPh_3)(PR_3)(\eta^6\text{-arene})]PF_6$, **1**, was achieved using the general route involving substitution of the labile acetonitrile ligand in the complex $[RuCl(NCMe)(PPh_3)(\eta^6\text{-arene})]PF_6$ (arene = *p*-cymene, **4a**; PhMe, **4b**), with the appropriate phosphine in CH_2Cl_2 at room temperature (Scheme 1).[11] Additionally, **1b** and **1f** were also prepared in high yield from reaction of triphenylphosphine with $[RuCl_2(PPh_3)(\eta^6\text{-arene})]$ and $[NH_4]PF_6$ in MeOH or CH_2Cl_2−MeOH, at slightly elevated temperatures. The synthesis of the bis-phosphine complex containing an anionic bidentate *ortho*-oxy-substituted triphenylphosphine, $[Ru(PPh_3)(\eta^2\text{-}PPh_2(C_6H_4O))(\eta^6\text{-}p\text{-cymene})]PF_6$, **2**, was accomplished in two steps, starting from the dinuclear ruthenium complex $[RuCl_2(\eta^6\text{-}p\text{-cymene})]_2$. Reaction of the dimer with the hydoxy-substituted phosphine and Cs_2CO_3 gave the chelate complex $[RuCl(\eta^2\text{-}PPh_2(C_6H_4O))(\eta^6\text{-}p\text{-cymene})]$, **5**, which then afforded **2** upon reaction with PPh_3 in EtOH under reflux followed by metathesis using $[NH_4]PF_6$ (Scheme 2). Complex **3** was prepared according to a literature protocol.[12]

The structures of these compounds are readily confirmed by $^{31}P\{^1H\}$ NMR spectroscopy. The spectra of the asymmetrical bis-phosphine complexes exhibit two doublets of equal intensity with large $^2J_{PP}$ couplings of ca. 52 Hz, whereas the coordinated phosphine resonances of the bis-triphenylphosphine compelxes **1b** and **1f** are observed as singlets; see Table 1. Chemical shifts of the coordinated PPh_3 ligand ranged from 20.3 to 31.9 ppm, with the signals at higher frequency corresponding to complexes containing $PPhMe_2$. The structures of these complexes are further corroborated by both ^1H and ^{13}C NMR spectroscopy. Of note, the signals of the C^4 atoms (see Schemes 1 and 2 for labeling) are generally found at higher frequency than the other arene atoms. This is indicative of reduced coordination of the arene and is in line with the large degree of steric bulk from the phosphine co-ligands (the effect is most pronounced in **1b**−**d**).

The solid-state structures of **1a**, **1c**, and **1d** have been determined by X-ray diffraction, depicted in Figure 1, and exhibit comparable structural parameters to the structures of **1b**·BF_4,[13] **1f**,[14] and **3**;[12] all contain large P−Ru−P angles of ca. 98° (see Table S1). As a consequence of the steric bulk in the coordination sphere, there is a significant elongation of the Ru−C4 bond lengths in comparison to the other Ru−C bonds for **1a**−**d** and **1f** (av Ru1−C4, 2.33 Å; av Ru1−C_{av}, 2.28 Å), in keeping with the ^{13}C NMR spectroscopic data (see above). The Ru1−C1 bond in **1d** is also significantly elongated [2.334(11) Å]. In comparison, there is no significant Ru−C bond lengthening observed in **3**, presumably due to the tethering of the arene. The coordination mode of *ortho*-oxy-substituted triphenylphosphine in **5** is further verified by X-ray crystallography (Figure 2).

2. Tandem Mass Spectrometry and Ligand Exchange Kinetics. ESI-MS of **1**−**3** in each case gave strong parent ion peaks with the expected isotope patterns. Collision-induced

(11) Chaplin, A. B.; Fellay, C.; Laurenczy, G.; Dyson, P. J. *Organometallics* **2007**, *26*, 586.

(12) Smith, P. D.; Gelbrich, T.; Hursthouse, M. B. *J. Organomet. Chem.* **2002**, *659*, 1.

(13) Lalrempuia, R.; Carroll, R. J.; Kollipara, M. R. *J. Coord. Chem.* **2003**, *56*, 1499.

(14) Polam, J. R.; Porter, L. C. *Inorg. Chim. Acta* **1993**, *205*, 119.

(15) In general, only qualitative trends can be made, as the collision energy is not well defined in CID MS/MS when using quadrupole ion trap instruments (ref 22a). Although it is possible to obtain quantitative gas phase dissociation energies using mass spectrometry (e.g., Hammad, L. A.; Gerdes, G.; Chen, P. *Organometallics* **2005**, *24*, 1907; Westmore, J. B.; Rosenberg, L.; Hooper, T. S.; Willett, G. D.; Fisher, K. J. *Organometallics* **2002**, *21*, 5688), the instruments required tend to be more elaborate and experiments are time intensive. This investigation demonstrates that useful trends can be extracted rapidly (e.g., ESI-MS/MS measurements in this work were completed in less than one day and under identical conditions) using a simple mass spectrometry method on common instrumentation.

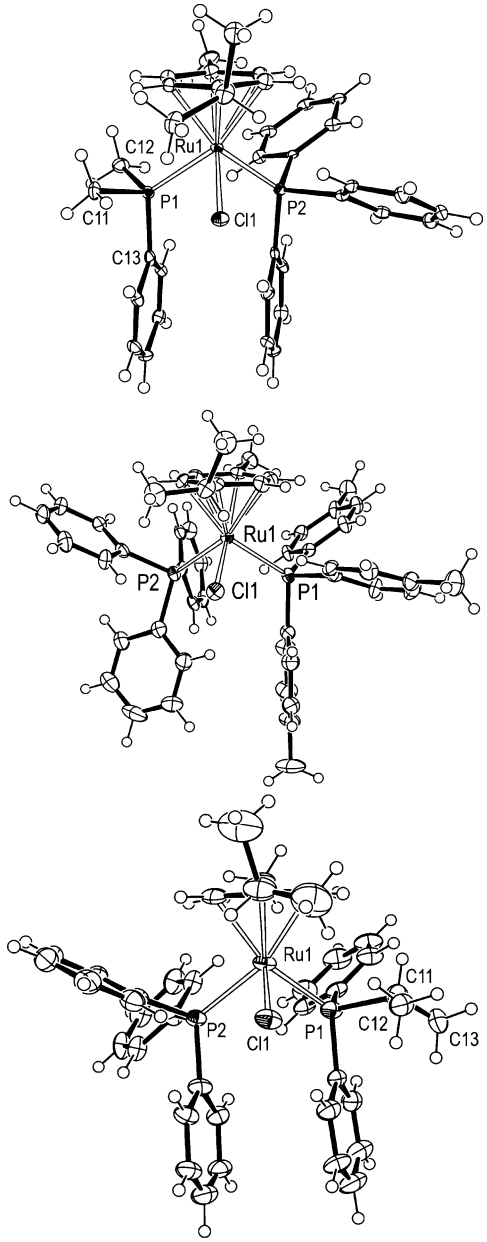

Figure 1. ORTEP representation of **1a** (top), **1c** (middle), and **1d** (bottom). Thermal ellipsoids are drawn at the 50% probability level. Solvent molecules and counter anions are omitted for clarity. Relevant bond parameters are given in Table 2.

dissociation (CID) of the PPh_3 ligand was found to be the primary pathway for the parent ions by ESI-MS/MS (Figure 3). To obtain a qualitative scale of PPh_3 dissociation energy, changes in the relative intensities of parent ion fragments were monitored as the normalized collision energy (*E*) was increased.[15,16] Changes in the fragmentation for **1b** with *E* are illustrated in Figure 4 , and data for this and the other complexes are compiled in Table 3. From inspection of these data, all recorded under identical conditions, several key trends can be

(16) The normalized collision energy (*E*) is a standardized collision energy scale based on the amplitude of the applied resonance excitation rf voltage (used for inducing fragmentation) and the mass of the parent ion. The amplitude of the rf voltage is given by $(E/0.3)(mb + a)$, where *m* (u) is the parent mass and *a* (V) and *b* (V/u) are instrument-dependent parameters (tick amp intercept and slope). This is a useful quantity, as it normalizes out the differences between instruments and the parent mass effect. More details can be found in: Lopez, L. L.; Tiller, P. R.; Senko, M. W.; Schwartz, J. C. *Rapid Commun. Mass Spectrom.* **1999**, *13*, 663.

Table 2. Key Bond Lengths (Å) and Angles (deg) for 1a, 1c, and 1d

	1a	1c	1d
Ru1−Cl1	2.414(2)	2.383(2)	2.397(3)
Ru1−P1	2.350(2)	2.369(2)	2.377(4)
Ru1−P2	2.372(2)	2.397(2)	2.395(3)
Ru1−C1	2.263(6)	2.308(6)	2.334(11)
Ru1−C4	2.326(6)	2.328(6)	2.325(12)
Ru1−C_{av}	2.28(3)	2.28(4)	2.28(5)
Cl1−Ru1−P1	83.68(6)	88.80(5)	89.77(11)
Cl1−Ru1−P2	88.45(6)	86.43(6)	83.04(11)
P1−Ru1−P2	97.10(6)	99.53(6)	98.15(11)

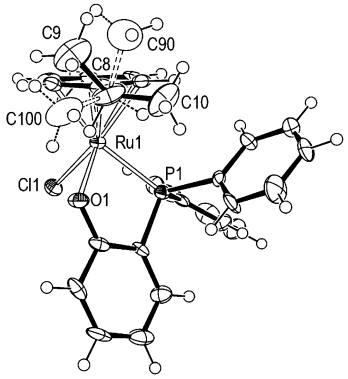

Figure 2. ORTEP representation of **5** (selected molecule from the asymmetric cell). Thermal ellipsoids are drawn at the 50% probability level. A disordered component of the *p*-cymene ring (C8, C90, C100) is shown with dashed bonds. Solvent molecule is omitted for clarity.

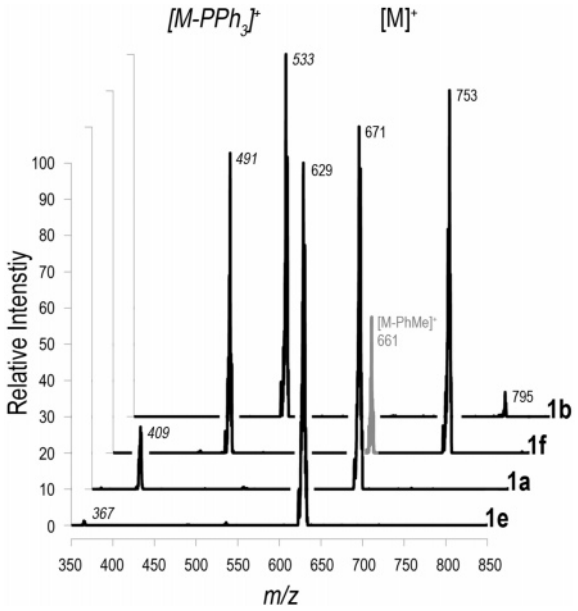

Figure 3. ESI-MS/MS of **1a**, **1b**, **1e**, and **1f** at 20% normalized collision energy [CH_2Cl_2, 80 °C, 5.0 kV].

established. First, as the steric bulk in the coordination sphere is increased, either by substitution on the arene ring (*p*-cymene > PhMe) or due to the steric bulk of the co-phosphine ($PPh_3 \approx P(p\text{-tol})_3 \approx PPh_2{}^iPr \gg PPhMe_2$), the Ru−$PPh_3$ bond is more readily fragmented. Second, fragmentation is reduced when rotation of the Ru−PR_3 bonds is restricted, such as in **2** and **3**. In addition to loss of PPh_3, additional fragmentation paths can be observed for **1d**−**f**. In the case of **1d**, $PPh_2{}^iPr$ loss is observed, while for both **1e** and **1f** arene loss can also be observed. Owing to the relatively high collision energy required

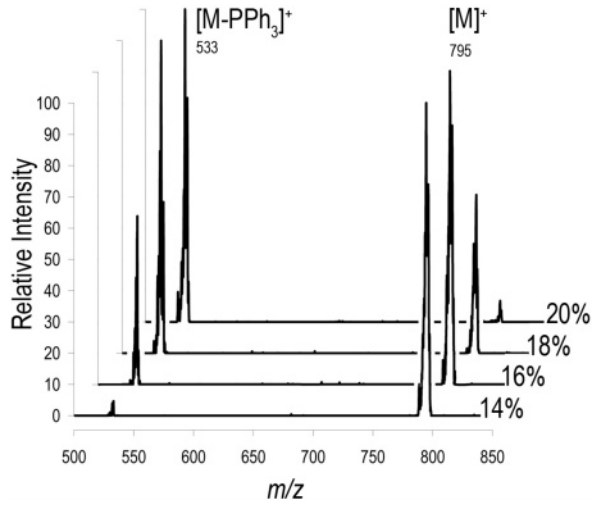

Figure 4. ESI-MS/MS of **1b** at different normalized collision energy [CH_2Cl_2, 80 °C, 5.0 kV].

Scheme 3. Exchange Kinetics of 1−3

$$[Ru]\text{-}(PPh_3)(PR_3) \xrightarrow[THF]{k_1,\ P(p\text{-tol})_3} [Ru]\text{-}(P(p\text{-tol})_3)(PR_3) \xrightarrow[THF]{k_2,\ P(p\text{-tol})_3} [Ru]\text{-}(P(p\text{-tol})_3)_2$$

to achieve dissociation of the PPh_3 ligand in **1e**, loss of $PPhMe_2$ also becomes significant.

The ease of PPh_3 loss, as shown by ESI-MS/MS, follows the order **1b** ≈ **1d** ≈ **1c** > **1f** > **1a** > **2** > **3** > **1e**. The lability of the PPh_3 ligand is further confirmed by supplementary experiments involving ligand exchange with P(*p*-tol)$_3$ under pseudo-first-order conditions (Scheme 3). Substitution of PPh_3 is observed for all of the bis-phosphine complexes at 60 °C, with the exception of **1e**, although the rate of exchange varies significantly; see Table 3. Substitution of $PPh_2{}^i$Pr is also observed for complex **1d**, although at much reduced rate compared to PPh_3 substitution ($t_{1/2}(1) = 37$ s vs $t_{1/2}(2) = 33$ min), consistent with the observed fragmentation pattern of this complex. No substitution of $PPhMe_2$ is observed for **1a** or **1e**. These data correlate well with those of the ESI-MS/MS, with **1b**−**d** showing the most rapid exchange, with an appreciable rate at room temperature (an example is given in Figure 5). The temperature dependence of the exchange reactions of **1b** and **1d** was determined and shows good Eyring behavior (Figure 6). The resulting activation parameters ($\Delta H^{\ddagger}$ ca. 112 kJ mol^{-1}, $\Delta S^{\ddagger}$ ca. +50 J mol^{-1} K^{-1}, Table 4) are consistent with a dissociative mechanism.[11,17]

Complex **1c** is also observed to undergo a related ligand exchange process in THF without added phosphine, in which

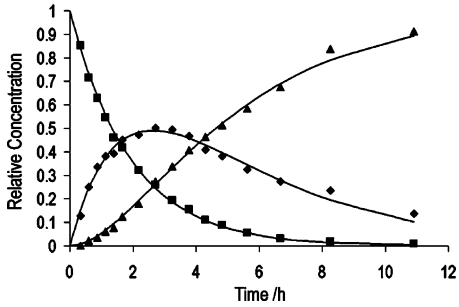

Figure 5. Exchange reaction of **1b** with P(*p*-tol)$_3$ in THF at 26 °C with kinetic fit: **1b** (■), **1c** (◆), [RuCl(P(*p*-tol)$_3$)$_2$(η^6-*p*-cymene)]$^+$, **6** (▲).[18]

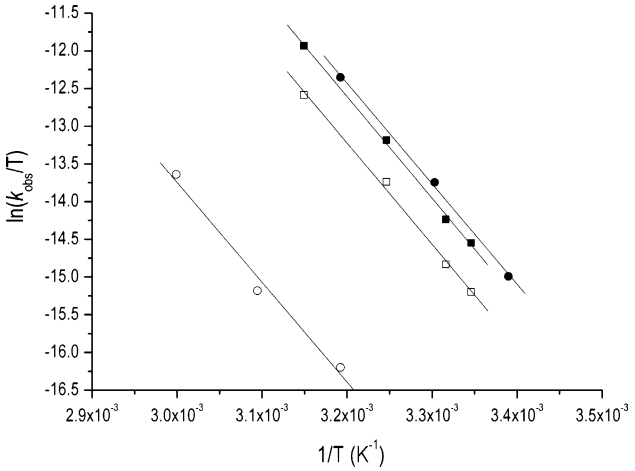

Figure 6. Eyring plots for the exchange reactions of **1b** (squares) and **1d** (circles). Filled and open points correspond to exchange 1 and 2, respectively.

exchange of both PPh_3 and P(*p*-tol)$_3$ results in a statistical mixture of the bis-phosphine complexes **1c**, **1b**, and [RuCl(P(*p*-tol)$_3$)$_2$(η^6-*p*-cymene)]PF_6 (**6**)[18] ($K = 0.25$, Scheme 4). This process occurs at an appreciable rate at room temperature, with the equilibrium composition reached in ca. 1 day (Figure 7). By following the rate of approach to equilibrium at different temperatures by $^{31}P\{^1H\}$ NMR spectroscopy the activation parameters for the forward and reverse reactions can be estimated (Table 5) and are similar to those determined for the exchange reactions described above. These parameters, together with the absence of free phosphine signals in the $^{31}P\{^1H\}$ NMR spectra during the equilibration, further suggest a dissociative mechanism and highlight the lability of the phosphine ligands in the complexes with sterically crowded coordination spheres.

Table 3. ESI-MS/MS, Kinetic, and Catalytic Data for 1−3

			ESI-MS/MS[a]		exchange (THF, 60 °C)[b]		catalysis
	arene	PR_3	$[M - PPh_3]^+/[M]^+$ ($E = 20\%$)	$E_{1/2}$[c]/%	$t_{1/2}(1)$	$t_{1/2}(2)$	$T_{100\%}$[d]/°C
1a	*p*-cymene	$PPhMe_2$	0.17	21.3	1.2 days		80
1b	*p*-cymene	PPh_3	14.3	16.0	43 s[e,f]		50
1c	*p*-cymene	P(*p*-tol)$_3$	5.6	16.6	80 s[f,g]		50
1d	*p*-cymene	$PPh_2{}^i$Pr	20.0[h]	16.2[i]	37 s[e,f]	33 min	50
1e	PhMe	$PPhMe_2$	0.01	23.9[j]	—[k]		80
1f	PhMe	PPh_3	0.81[l]	19.4[m]	57 min[e]	86 min[e]	60
2	*p*-cymene	$PPh_2(C_6H_4O)$	0.08	22.0	3.4 days		90
3		$Ph(CH_2)_3PPh_2$	0.07	22.3	>3 days		90

[a] ESI-MS/MS conditions: CH_2Cl_2, 80 °C, spray voltage 5.0 kV. [b]Exchange with P(*p*-tol)$_3$ (20 equiv). [c]E required to obtain a relative intensity for [M − PPh_3] of 50%. Error ± 0.2%. [d]Temperature required for 100% conversion of styrene to ethyl benzene under the catalytic conditions: 5.0×10^{-6} mol of precatalyst, S:C = 2000:1, 60 min, 2 mL of THF, 50 bar of H_2, 100 mg of octane added as internal standard. Conversions determined by GC (values reported as average of at least three experiments). [e]30 equiv of P(*p*-tol)$_3$. [f]Extrapolated from lower temperature data. [g]From second exchange with PPh_3 in **1b**. [h][M − $PPh_2{}^i$Pr] (35%) observed. [i][M − $PPh_2{}^i$Pr] (17%) observed. [j][M − PhMe] (35%) and [M − $PPhMe_2$] (7%) observed. [k]No exchange detected after ca. 60 h. [l][M − PhMe] (35%) observed. [m][M − PhMe] (24%) observed.

Table 4. Activation Parameters for the Exchange Reactions of 1b and 1d[a]

	rxn	$\Delta H^{\ddagger}$/kJ mol^{-1}	$\Delta S^{\ddagger}$/J mol^{-1} K^{-1}	R^2_{fit}
1b	1	112 ± 3	+56 ± 10	0.998
	2[b]	112 ± 5	+50 ± 20	0.996
1d	1	111 ± 4	+54 ± 14	0.999
	2	110 ± 14	+20 ± 40	0.985

[a] THF, 30 equiv of P(*p*-tol)$_3$. Errors originate from the standard errors from linear fits of ln(k_{obs}/T) versus 1/*T*, i.e., $\sigma(\Delta H^{\ddagger}) = R\sigma$(slope), $\sigma(\Delta S^{\ddagger}) = R\sigma$(intercept). [b]Corresponds to single ligand exchange of **1c**.

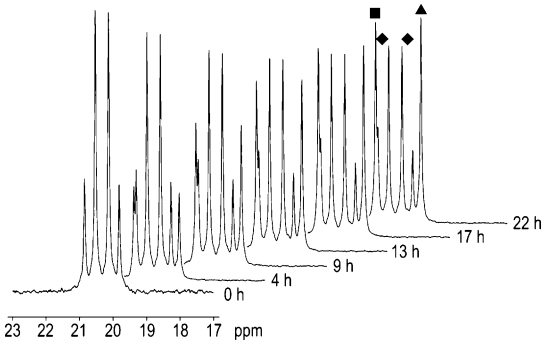

Figure 7. Equilibration of **1c** (◆; 20.7, 20.0 ppm, $^2J_{PP}$ = 52 Hz) in THF at 22 °C, **1b** (20.9 ppm; ■), and **6** (19.6 ppm; ▲).

Scheme 4. Equilibration of 1c

$$2[\text{Ru}]\text{-}(PPh_3)(P(p\text{-tol})_3) \underset{k_{-3}}{\overset{k_3}{\rightleftharpoons}} [\text{Ru}]\text{-}(PPh_3)_2 + [\text{Ru}]\text{-}(P(p\text{-tol})_3)_2$$

1c (THF) **1b** **6**

Table 5. Activation Parameters for the Equilibration of 1c in THF[a]

rxn	$\Delta H^{\ddagger}$/kJ mol^{-1}	$\Delta S^{\ddagger}$/J mol^{-1} K^{-1}	R^2_{fit}
3	116 ± 8	+40 ± 30	0.995
−3	116 ± 8	+50 ± 30	0.995

[a] Errors originate from the standard errors from linear fits of ln(k_{obs}/T) versus 1/*T* [i.e., $\sigma(\Delta H^{\ddagger}) = R\sigma$(slope), $\sigma(\Delta S^{\ddagger}) = R\sigma$(intercept).

Table 6. Catalytic Activity of 1−3, 7, and 8[a]

	conversion/%						
complex	30 °C	40 °C	50 °C	60 °C	70 °C	80 °C	90 °C
1a				0(3)	22(4)	100	
1b		74(8)	100				
1c	10(5)	60(7)	100				
1d	5(3)	54(11)	100				
1e				1(3)	3(3)	100	
1f		1(3)	5(4)	100			
2					0(3)	32(17)	100
3					0(3)	57(30)	100
7					2(3)	70(3)	100
8					2(3)	3(3)	5(3)

[a] Conditions: 5.0 × 10^{-6} mol of catalyst, S:C = 2000:1, 60 min, 2 mL of THF, 50 bar of H_2, 100 mg of octane added as internal standard. Conversions determined by GC. Values reported as average of at least three experiments; estimated error given in parentheses.

The catalytic activity of the bis-phosphine complexes **1**−**3** was investigated as a function of temperature, in 10 °C increments, for the hydrogenation of styrene in THF (50 bar of H_2, 60 min). These data are listed in Table 6, with the temperature corresponding to 100% conversation also listed in Table 3. The activity follows the order **1b** ≈ **1c** ≈ **1d** > **1f** > **1a** > **1e** > **2** ≈ **3**. A good correlation is found between the ESI-MS/MS data and the catalytic activity (Figure 8). Notably, **1b**−**d** show the highest activity (active at $T \leq 50$ °C). The catalytic activity increases with more bulky arene (**1a** > **1e**; **1b** > **1f**) and phosphine (**1b** > **1c** ≈ **1d** ≫ **1a**; **1f** > **1e**) ligands. In agreement with the ESI-MS/MS data, **2** and **3** require higher temperatures to observe catalytic activity, showing a similar temperature dependence to the related complex [RuCl(η^2-dppm)(η^6-*p*-cymene)]PF_6 (**7**) (active at $T \geq 80$ °C).[19] For comparison the neutral complex [$RuCl_2(PPh_3)(\eta^6$-*p*-cymene)] (**8**)[20] remains essentially inactive up to 90 °C.

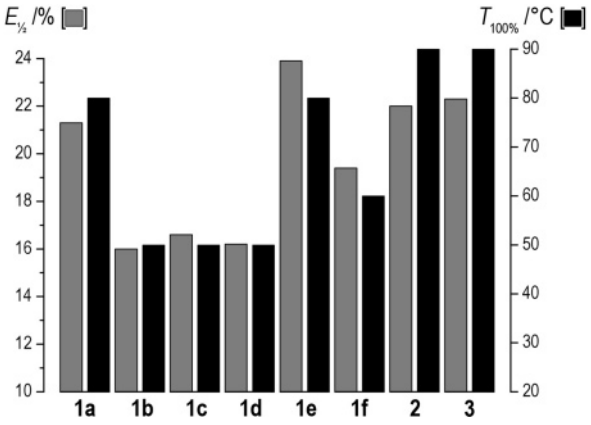

Figure 8. Correlation of catalytic activity (see Table 3, footnote d) with relative fragmentation energy determined by ESI-MS/MS (see Table 3, footnote c).

3. Concluding Remarks. The phosphine dissociation characteristics of a range of bis-phosphine ruthenium(II)−arene complexes have been investigated in both the gas and solution phase using tandem electrospray ionization mass spectrometry (ESI-MS/MS) and ligand exchange kinetics, respectively. Using this combination of techniques a number of trends in reactivity are firmly established, which are generally steric in origin, apparent to some degree from NMR and solid-state characterization, and show good correlation with the observed catalytic activity. Furthermore, the good agreement between these two properties suggests that phosphine dissociation is the rate-determining step for the generation of the active catalytic species. The most active catalyst precursors show good activity under comparably mild conditions (TOF ≥ 2000 h^{-1} for styrene hydrogenation in THF at 50 °C under 50 bar of H_2).

In particular, ESI-MS/MS proved to be an effective tool in assessing the catalytic activity by establishing reliable qualitative trends in phosphine dissociation energy. The correlation is especially satisfying owing to the simplicity of the mass spectrometry method, avoiding the necessity for quantitative phosphine dissociation measurements. Therefore this technique may be suitable, more generally, for rapid catalyst screening of other transition metal systems, naturally charged or with "electrospray friendly" ligands,[21] involving ligand dissociation as a rate-determining step. ESI-MS as a tool for catalyst

(17) (a) Bunten, K. A.; Farrar, D. H.; Poë, A. J.; Lough, A. J. *Organometallics* **2000**, *19*, 3674. (b) Serron, S. A.; Nolan, S. P. *Organometallics* **1995**, *14*, 4611. (c) Dias, P. B.; Minas de Piedade, M. E.; Simões, J. A. M. *Coord. Chem. Rev.* **1994**, *135*−*136*, 737.

(18) Complex **6** has been prepared for reference. A method similar to that of **1b** was used (see Experimental Section for full details).

(19) Jensen, S. B.; Rodger, S. J.; Spicer, M. D. *J. Organomet. Chem.* **1998**, *556*, 151.

(20) Bennett, M. A.; Smith, A. K. *J. Chem. Soc., Dalton Trans.* **1974**, 233.

(21) (a) Farrer, N. J.; McDonald, R.; McIndoe, J. S. *Dalton Trans.* **2006**, 4570. (b) Evans, C.; Nicholson, B. K. *J. Organomet. Chem.* **2003**, *665*, 95. (c) Decker, C.; Henderson, W.; Nicholson, B. K. *J. Chem. Soc., Dalton Trans.* **1999**, 3507.

Scheme 5

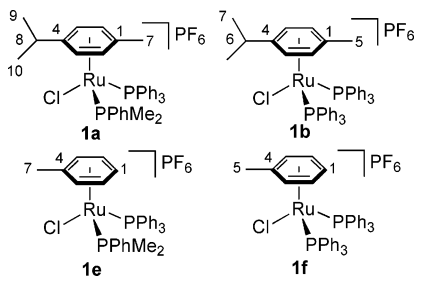

screening is an area of current interest,[22] although this particular application appears to be novel.

Experimental Section

All organometallic manipulations were carried out under a nitrogen atmosphere using standard Schlenk techniques. CH_2Cl_2 and THF were dried catalytically under dinitrogen using a solvent purification system, manufactured by Innovative Technology Inc. All other solvents were p.a. quality and saturated with nitrogen prior to use. [RuCl(NCMe)(PPh_3)(η^6-*p*-cymene)]PF_6,[11] [$RuCl_2$(PPh_3)(η^6-*p*-cymene)],[20] [$RuCl_2$(η^6-PhMe)]$_2$,[20] [$RuCl_2$(η^6-*p*-cymene)]$_2$,[20] *ortho*-$PPh_2(C_6H_4OH)$,[23] and [Ru(PPh_3)(η^7-$PPh_2(CH_2)_3$-Ph)]PF_6[12] were prepared as described elsewhere. [RuCl(η^2-dppm)(η^6-*p*-cymene)]PF_6 was prepared by metathesis of [RuCl(η^2-dppm)(η^6-*p*-cymene)]Cl in a similar manner as previously described for [RuCl(η^2-dppm)(η^6-*p*-cymene)]BF_4 (ref 2c); NMR data were in agreement with the literature.[19] All other chemicals are commercial products and were used as received. Spectra were recorded with a Bruker Avance 400 spectrometer at room temperature, unless otherwise stated. Chemical shirts are given in ppm and coupling constants (*J*) in Hz. The NMR labeling for complex **2** is given in Scheme 2; all other complexes are labeled similarly (see Scheme 5 for some examples). ESI-MS were recorded on a Thermo Finnigan LCQ DecaXP Plus quadrupole ion trap instrument. CH_2Cl_2 was used as the solvent for all experiments with a capillary temperature of 80 °C and spray voltage of 5.0 kV. The instrument parameters *a* and *b* for the ESI-MS/MS experiments[16] were 0.001080 V and 0.460908 V/u, respectively. Microanalyses were performed at the EPFL.

Preparation of [RuCl($PPhMe_2$)(PPh_3)(η^6-*p*-cymene)]PF_6 (1a). To a solution of [RuCl(NCMe)(PPh_3)(η^6-*p*-cymene)]PF_6 (0.50 g, 0.70 mmol) in CH_2Cl_2 (30 mL) was added $PPhMe_2$ (0.4 mL, 2.81 mmol), and the solution was stirred at RT for 30 min. The product was precipitated by the addition of excess diethyl ether (ca. 150 mL) and the precipitate washed with diethyl ether (2 × 50 mL). Yield: 0.54 g (96%) as a yellow powder. Orange crystals suitable for X-ray diffraction were obtained from a solution of $CHCl_3$ layered with toluene and pentane at 4 °C. ^{1}H NMR ($CDCl_3$): δ 7.40−7.75 (m, 20H, PPh), 5.90 (dd, $^3J_{HH}$ = 6.0, $^3J_{PH}$ = 3, 1H, H^6), 5.46 (d, $^3J_{HH}$ = 5.6, 1H, H^3), 5.02 (dd, $^3J_{HH}$ = 6.0, $^3J_{PH}$ = 5, 1H, H^2), 4.94 (d, $^3J_{HH}$ = 6.4, 1H, H^5), 2.58 (sept, $^3J_{HH}$ = 7.0, 1H, H^8), 1.60 (d, $^2J_{PH}$ = 10, 3H, PMe), 1.29 (s, 3H, H^7), 1.22 (d, $^2J_{PH}$ = 11, 3H, PMe′), 1.10 (d, $^3J_{HH}$ = 7.0, 3H, H^9), 1.10 (d, $^3J_{HH}$ = 7.0, 3H, H^{10}). ^{13}C{^{1}H} NMR ($CDCl_3$): δ 139.0 (d, $^1J_{PC}$ = 48, $PPhMe_2$), 134.5 (d, $^{2/3}J_{PC}$ = 9, PPh_3), 133.5 (d, $^1J_{PC}$ = 47, PPh_3), 131.3 (d, $^4J_{PC}$ = 2, PPh_3), 130.8 (d, $^4J_{PC}$ = 3, P*Ph*Me_2), 129.4 (d, $^{2/3}J_{PC}$ = 8, P*Ph*Me_2), 129.2 (d, $^{3/2}J_{PC}$ = 10, $PPhMe_2$), 128.7 (d, $^{3/2}J_{PC}$ = 10, PPh_3), 128.0 (dd, $^2J_{PC}$ = $^2J_{PC}$ = 3, C^4), 99.0 (s, C^1), 97.7 (d, $^2J_{PC}$ = 4, C^6), 96.4 (d, $^2J_{PC}$ = 3, C^2), 90.7 (d, $^2J_{PC}$ = 9, C^3), 89.1 (d, $^2J_{PC}$ = 10, C^5), 30.9 (s, C^8), 21.7 (s, $C^{9/10}$), 21.1 (s, $C^{10/9}$), 16.5 (s, C^7), 15.1 (d, $^1J_{PC}$ = 36, PMe′), 15.1 (d, $^1J_{PC}$ = 33, PMe). ^{31}P{^{1}H} NMR ($CDCl_3$): δ 27.0 (d, $^2J_{PP}$ = 54, 1P, $RuPPh_3$), 3.5 (d, $^2J_{PP}$ = 54, 1P, $RuPPhMe_2$), −144.1 (sept, $^1J_{PF}$ = 713, 1P, *P*F_6). ESI-MS (CH_2Cl_2) positive ion: *m/z* 671 $[M]^+$; negative ion: *m/z* 145 $[PF_6]^-$. Anal. Calcd for $C_{36}H_{40}ClF_6P_3Ru$ (816.15 g mol^{-1}): C, 52.98; H, 4.94. Found: C, 52.97; H, 4.75.

Preparation of [RuCl(PPh_3)$_2$(η^6-*p*-cymene)]PF_6 (1b). Method A: A suspension of [$RuCl_2$(PPh_3)(η^6-*p*-cymene)] (0.300 g, 0.53 mmol), PPh_3 (0.277 g, 1.06 mmol), and $[NH_4]PF_6$ (0.061 g, 0.58 mmol) in MeOH (20 mL) was stirred at 35 °C for 2 h. The solvent was removed in vacuo and the residue extracted through Celite with CH_2Cl_2 (ca. 20 mL). The product was then isolated, as a yellow powder, by precipitation with pentane and washed with EtOH (10 mL) and pentane (2 × 10 mL). Yield: 0.39 g (78%).

Method B: A solution of [RuCl(NCMe)(PPh_3)(η^6-*p*-cymene)]PF_6 (1.00 g, 1.39 mmol) and PPh_3 (1.09 g, 4.16 mmol) in CH_2Cl_2 (40 mL) was stirred at RT for 3 h. The product was precipitated by the addition of excess diethyl ether (ca. 200 mL) and washed with diethyl ether (2 × 40 mL). Purification by precipitation from CH_2Cl_2 by addition of pentane gave the pure product as a yellow powder. Yield: 1.07 g (82%). NMR data are in agreement with the literature,[13] although a more thorough characterization is included here. ^{1}H NMR ($CDCl_3$): δ 7.13−7.54 (m, 30H, PPh), 5.55−5.67 (m, 2H, H^2), 5.07 (d, $^3J_{HH}$ = 6.1, 1H, H^3), 2.72 (sept, $^3J_{HH}$ = 6.9, 1H, H^6), 1.25 (d, $^3J_{HH}$ = 7.0, 6H, H^7), 1.10 (s, 3H, H^5). ^{13}C{^{1}H} NMR ($CDCl_3$): δ 127−135 (m, PPh), 131.8 (C^4), 100.7 (s, C^1), 97.4 (t, $^2J_{PC}$ = 2, C^2), 89.1 (t, $^2J_{PC}$ = 5, C^3), 31.5 (s, C^6), 21.4 (s, C^7), 15.3 (s, C^5). ^{31}P{^{1}H} NMR ($CDCl_3$): δ 20.8 (s, 2P), −144.4 (sept, $^1J_{PF}$ = 713, 1P, PF_6). ESI-MS (CH_2Cl_2) positive ion: *m/z* 795 $[M]^+$; negative ion: *m/z* 145 $[PF_6]^-$.

Preparation of [RuCl(P(*p*-C_6H_4Me)$_3$)(PPh_3)(η^6-*p*-cymene)]PF_6 (1c). A solution of [RuCl(NCMe)(PPh_3)(η^6-*p*-cymene)]PF_6 (0.50 g, 0.70 mmol) and P(*p*-$C_6H_4Me)_3$ (2.50 g, 8.21 mmol) in CH_2Cl_2 (50 mL) was stirred at RT for 30 min. The product was precipitated by the addition of excess diethyl ether (ca. 150 mL) and the precipitate washed with diethyl ether (2 × 50 mL). Purification by precipitation twice from CH_2Cl_2−pentane gave the pure product as a yellow powder. Yield: 0.46 g (67%). Orange crystals suitable for X-ray diffraction were obtained by recrystallization from a mixture of CH_2Cl_2, toluene, and pentane at −20 °C. ^{1}H NMR ($CDCl_3$): δ 6.93−7.53 (m, 27H, PPh + H^{12} + H^{13}), 5.57−5.64 (m, 1H, H^2), 5.48−5.57 (m, 1H, H^6), 5.13 (d, $^3J_{HH}$ = 6.1, 1H, H^3), 5.00 (d, $^3J_{HH}$ = 6.1, 1H, H^5), 2.71 (sept, $^3J_{HH}$ = 6.8, 1H, H^8), 2.37 (s, 9H, H^{15}), 1.26 (d, $^3J_{HH}$ = 6.8, 3H, H^9), 1.22 (d, $^3J_{HH}$ = 6.8, 3H, H^{10}), 1.07 (s, 3H, H^7). ^{13}C{^{1}H} NMR ($CDCl_3$, selected peaks only): δ 134 (C^4), 100 (C^1), 97 (C^2), 96 (C^6), 89 (C^3), 89 (C^5). ^{31}P{^{1}H} NMR ($CDCl_3$): δ 20.3 (d, $^2J_{PP}$ = 52, 1P, $RuPPh_3$), 19.8 (d, $^2J_{PP}$ = 52, 1P, Ru*P*(*p*-tol)$_3$), −144.3 (sept, $^1J_{PF}$ = 713, 1P, PF_6). ESI-MS (CH_2Cl_2) positive ion: *m/z* 837 $[M]^+$; negative ion: *m/z* 145 $[PF_6]^-$. Anal. Calcd for $C_{49}H_{50}ClF_6P_3Ru$ (982.37 g mol^{-1})·2/3(Et_2O): C, 60.15; H, 5.54. Found: C, 60.43; H, 5.28.

Preparation of [RuCl(PPh_2*i*Pr)(PPh_3)(η^6-*p*-cymene)]PF_6 (1d). A solution of [RuCl(NCMe)(PPh_3)(η^6-*p*-cymene)]PF_6 (0.50 g, 0.70 mmol) and PPh_2*i*Pr (0.48 g, 2.09 mmol) in CH_2Cl_2 (20 mL) was stirred at RT for 2.5 h. The product was precipitated by the addition of excess diethyl ether (ca. 100 mL) and the precipitate washed with diethyl ether (2 × 50 mL). Recrystallization from CH_2Cl_2−pentane gave the product as orange crystals. Yield: 0.36 g (58%). Orange crystals suitable for X-ray diffraction were obtained by recrystallization from CH_2Cl_2−pentane at −20 °C. ^{1}H NMR ($CDCl_3$): δ 7.00−7.85 (m, 25H, PPh), 6.13 (dd, $^3J_{HH}$ = 6.2, $^3J_{PH}$ = 5, 1H, H^6), 5.81 (d, $^3J_{HH}$ = 6.1, 1H, H^5), 5.31 (dd, $^3J_{HH}$ = 6.2, $^3J_{PH}$ = 5, 1H, H^2), 4.44 (d, $^3J_{HH}$ = 5.6, 1H, H^3), 2.68 (br, 1H, H^{11}), 2.60 (sept, $^3J_{HH}$ = 7.0, 1H, H^8), 1.29 (d, $^3J_{HH}$ = 7.0, 3H, H^9), 0.96−1.12 (obscured, 3H, H^{12}), 1.07 (d, $^3J_{HH}$ = 7.0, 3H, H^{10}), 1.02 (s,

(22) (a) Henderson, W.; McIndoe, J. S. *Mass Spectrometry of Inorganic, Coordination and Organometallic Compounds: Tools−Techniques−Tricks*; John Wiley & Sons: Chichester, 2005. (b) Markert, C.; Pfalz, A. *Angew. Chem., Int. Ed.* **2004**, *43*, 2498. (c) Chen, P. *Angew. Chem., Int. Ed.* **2003**, *42*, 2832.

(23) Ainscough, E. W.; Brodie, A. M.; Chaplin, A. B.; O'Connor, J. M.; Otter, C. *Dalton Trans.* **2006**, 1264.

3H, H^7), (d, $^3J_{PH}$ = 15, $^3J_{HH}$ = 6.6, 3H, H^{13}). ^{13}C{^{1}H} NMR ($CDCl_3$): δ 126−136 (m, PPh), 132 (C^4), 99.6 (br, C^6), 98.8 (s, C^1), 95.7 (d, $^2J_{PC}$ = 3, C^2), 87.5 (d, $^2J_{PC}$ = 10, C^3), 85.5 (d, $^2J_{PC}$ = 10, C^5), 31.4 (s, C^8), 31.0 (d, $^1J_{PH}$ = 25, H^{11}), 21.7 (s, C^9), 21.0 (s, C^{10}), 19.4 (d, $^2J_{PC}$ = 4, C^{13}), 18.6 (s, C^{12}), 15.5 (s, C^7). ^{31}P{^{1}H} NMR ($CDCl_3$): δ 23.5 (d, $^2J_{PP}$ = 50, 1P, $RuPPh_3$), 18.8 (d, $^2J_{PP}$ = 50, 1P, $RuPPh_2{}^i$Pr), −144.2 (sept, $^1J_{PF}$ = 713, 1P, PF_6). ESI-MS (CH_2Cl_2) positive ion: *m/z* 761 $[M]^+$; negative ion: *m/z* 145 $[PF_6]^-$. Anal. Calcd for $C_{43}H_{46}ClF_6P_3Ru$(906.27 g mol^{-1})·3/4(CH_2Cl_2): C, 54.17; H, 4.94. Found: C, 54.45; H, 4.70.

Preparation of [$RuCl_2(PPh_3)(\eta^6$-PhMe)]. A solution of [$RuCl_2(\eta^6$-PhMe)]$_2$ (0.50 g, 0.95 mmol) and PPh_3 (0.62 g, 2.36 mmol) in CH_2Cl_2 (20 mL) was stirred at RT for 90 min. The product was then precipitated by the addition of hexane and washed with diethyl ether (2 × 10 mL) and then pentane (2 × 10 mL). Yield: 0.86 g (86%) as an orange powder. ^{1}H NMR ($CDCl_3$): δ 7.76 (t, $^3J_{HH}$ = 8.8, 6H, PPh), 7.34−7.50 (m, 9H, PPh), 5.18−5.28 (m, 4H, H^2 + H^3), 4.58 (t, $^3J_{HH}$ = 5.0, 1H, H^1), 2.28 (s, 3H, H^5). ^{13}C{^{1}H} NMR ($CDCl_3$): δ 134.2 (d, $^{2/3}J_{PC}$ = 9, PPh_3), 130.4 (d, $^4J_{PC}$ = 2, PPh_3), 128.1 (d, $^{3/2}J_{PC}$ = 10, PPh_3), 108.7 (d, $^2J_{PC}$ = 6, C^4), 89.0 (br, C^2), 88.8 (d, $^2J_{PC}$ = 6, C^3), 81.3 (s, C^1), 18.7 (s, C^5). ^{31}P{^{1}H} NMR ($CDCl_3$): δ 28.2 (s, 1P). Anal. Calcd for $C_{25}H_{23}Cl_2PRu$ (526.41 g mol^{-1}): C, 57.04; H, 4.40. Found: C, 56.65; H, 4.14.

Preparation of [$RuCl(NCMe)(PPh_3)(\eta^6$-PhMe)]PF_6 (4b). A suspension of [$RuCl_2(PPh_3)(\eta^6$-PhMe)] (0.8 g, 1.52 mmol) and [NH_4]PF_6 (0.32 g, 1.96 mmol) in CH_3CN (40 mL) was heated at reflux for 2 h. The solution was cooled to RT and the solvent removed in vacuo. The residue was then extracted with CH_2Cl_2 (50 mL) through Celite. Recrystallization from CH_2Cl_2−diethyl ether removed a small amount of red-purple impurity. Yield: 0.89 g (85%) as a yellow powder of ∼95% purity. ^{1}H NMR ($CDCl_3$): δ 7.45−7.63 (m, 15H, PPh_3), 6.01 (d, $^3J_{HH}$ = 5.9, 1H, H^3), 5.86−5.94 (m, 1H, H^2), 5.42 (d, $^3J_{HH}$ = 5.7, 1H, H^5), 5.30−5.37 (m, 1H, H^6), 4.85 (t, $^3J_{HH}$ = 5.2, 1H, H^3), 2.37 (s, 3H, H^7), 1.97 (s, 3H, NCMe). ^{13}C{^{1}H} NMR ($CDCl_3$): δ 134.1 (d, $^{2/3}J_{PC}$ = 10, PPh_3), 131.5 (d, $^4J_{PC}$ = 3, PPh_3), 130.4 (d, $^1J_{PC}$ = 51, PPh_3), 128.9 (d, $^{3/2}J_{PC}$ = 11, PPh_3), 127.2 (s, NCMe), 114.5 (d, $^2J_{PC}$ = 6, C^4), 93.0 (br, C^2), 91.4 (d, $^2J_{PC}$ = 8, C^3), 89.6 (s, C^6), 86.6 (d, $^2J_{PC}$ = 2, C^5), 84.7 (s, C^1), 19.0 (s, C^7), 3.3 (s, NCMe). ^{31}P{^{1}H} NMR ($CDCl_3$): δ 35.6 (s, 1P), −144.2 (sept, $^1J_{PF}$ = 713, 1P, PF_6). ESI-MS (CH_2Cl_2) positive ion: *m/z* 491 (29%) $[M - MeCN]^+$, 532 $[M]^+$; negative ion: *m/z* 145 $[PF_6]^-$.

Preparation of [$RuCl(PPhMe_2)(PPh_3)(\eta^6$-PhMe)]$PF_6$ (1e). To a solution of [$RuCl(NCMe)(PPh_3)(\eta^6$-PhMe)]PF_6 (0.30 g, 0.44 mmol) in CH_2Cl_2 (5 mL) was added $PPhMe_2$ (0.25 mL, 1.76 mmol), and the solution was stirred at RT for 5 min. The product was precipitated by the addition of excess diethyl ether (ca. 50 mL) and the precipitate washed with diethyl ether (2 × 10 mL) and pentane (2 × 10 mL). Yield: 0.23 g (67%) as a yellow powder. ^{1}H NMR ($CDCl_3$): δ 7.45−7.82 (m, 20H, PPh), 5.83−5.90 (m, 1H, H^2), 5.47 (d, $^3J_{HH}$ = 6.4, 1H, H^5), 5.26−5.34 (m, 1H, H^6), 4.68 (t, $^3J_{HH}$ = 5.6, 1H, H^1), 4.28 (d, $^3J_{HH}$ = 5.6, 1H, H^3), 2.04 (d, $^2J_{PH}$ = 10, 3H, PMe), 2.00 (s, 3H, H^7), 0.76 (d, $^2J_{PH}$ = 11, 3H, PMe′). ^{13}C{^{1}H} NMR ($CDCl_3$): δ 142.4 (d, $^1J_{PC}$ = 50, $PPhMe_2$), 134.4 (d, $^{2/3}J_{PC}$ = 10, PPh_3), 132.9 (d, $^1J_{PC}$ = 48, PPh_3), 131.6 (d, $^4J_{PC}$ = 2, PPh_3), 130.6 (d, $^4J_{PC}$ = 3, $PPhMe_2$), 129.2 (d, $^{2/3}J_{PC}$ = 10, $PPhMe_2$), 128.9 (d, $^{3/2}J_{PC}$ = 10, PPh_3), 128.7 (d, $^{3/2}J_{PC}$ = 8, $PPhMe_2$), 118.0 (dd, $^2J_{PC}$ = 4, $^2J_{PC}$ = 2, C^4), 97.2 (d, $^2J_{PC}$ = 9, C^3), 96.9 (d, $^2J_{PC}$ = 4, C^6), 95.1 (d, $^2J_{PC}$ = 2, C^2), 94.5 (d, $^2J_{PC}$ = 10, C^5), 84.0 (s, C^1), 18.8 (s, C^7), 17.0 (d, $^1J_{PC}$ = 34, PMe), 12.2 (d, $^1J_{PC}$ = 36, PMe′). ^{31}P{^{1}H} NMR ($CDCl_3$): δ 31.9 (d, $^2J_{PP}$ = 56, 1P, $RuPPh_3$), 3.7 (d, $^2J_{PP}$ = 56, 1P, $RuPPhMe_2$), −144.1 (sept, $^1J_{PF}$ = 713, 1P, PF_6). ESI-MS (CH_2Cl_2) positive ion: *m/z* 629 $[M]^+$; negative ion: *m/z* 145 $[PF_6]^-$. Anal. Calcd for $C_{33}H_{34}ClF_6P_3Ru$ (774.07 g mol^{-1}): C, 51.21; H, 4.43. Found: C, 51.53; H, 4.38.

Preparation of [$RuCl(PPh_3)_2(\eta^6$-PhMe)]PF_6 (1f). Method A: A solution of [$RuCl_2(PPh_3)(\eta^6$-PhMe)] (0.50 g, 0.95 mmol), PPh_3 (0.28 g, 1.07 mmol), and [NH_4]PF_6 (0.19 g, 1.14 mmol) in 1:1 MeOH−CH_2Cl_2 (50 mL) was stirred at 35 °C for 2 h, then at 50 °C for 2 h. The solution was concentrated, giving a yellow solid, which was filtered and washed with EtOH (2 × 30 mL) and then diethyl ether (3 × 20 mL). Yield: 0.59 g (69%) as a yellow powder.

Method B: A solution of [$RuCl(NCMe)(PPh_3)(\eta^6$-PhMe)]PF_6 (0.10 g, 0.15 mmol) and PPh_3 (0.12 g, 0.46 mmol) in CH_2Cl_2 (5 mL) was stirred at RT for 3 h. The product was precipitated by the addition of excess diethyl ether (ca. 50 mL) and the precipitate washed with diethyl ether (2 × 10 mL) and pentane (2 × 10 mL). Yield: 0.10 g (75%). ^{1}H NMR ($CDCl_3$): δ 7.20−7.35 (m, 18H, PPh_3), 7.35−7.50 (m, 12H, PPh_3), 5.73−5.82 (m, 2H, H^2), 5.05 (t, $^3J_{HH}$ = 5.4, 1H, H^1), 4.69 (d, $^3J_{HH}$ = 6.0, 2H, H^3), 2.11 (s, 3H, H^5). ^{13}C{^{1}H} NMR ($CDCl_3$): δ 133.9 (t, $^{2/3}J_{PC}$ = 5, PPh_3), 131.0 (br, PPh_3), 128.5 (t, $^{3/2}J_{PC}$ = 5, PPh_3), 122.6 (t, $^2J_{PC}$ = 3, C^4), 98.3 (br, C^2), 94.6 (t, $^2J_{PC}$ = 5, C^3), 83.5 (s, C^1), 19.2 (s, C^5). ^{31}P{^{1}H} NMR ($CDCl_3$): δ 22.4 (s, 1P, $RuPPh_3$), −144.3 (sept, $^1J_{PF}$ = 713, 1P, PF_6). ESI-MS (CH_2Cl_2) positive ion: *m/z* 753 $[M]^+$; negative ion: *m/z* 145 $[PF_6]^-$. Anal. Calcd for $C_{43}H_{38}ClF_6P_3Ru$(898.21 g mol^{-1})·1/2(CH_2Cl_2): C, 55.54; H, 4.18. Found: C, 55.27; H, 4.12.

Preparation of [$RuCl(\eta^2$-PPh_2(*o*-C_6H_4O))(η^6-*p*-cymene)] (5). A suspension of [$RuCl_2(\eta^6$-*p*-cymene)]$_2$ (1.50 g, 2.45 mmol), PPh_2(*o*-C_6H_4OH) (1.44 g, 5.17 mmol), and Cs_2CO_3 (0.80 g, 2.45 mmol) in MeOH (100 mL) was heated at reflux for 1 h. The solution was cooled to RT and the solvent removed in vacuo. The residue was extracted with CH_2Cl_2 (60 mL) through Celite and hexane (ca. 60 mL) added. Concentration, followed by cooling to −20 °C, gave the product as an orange-red crystalline solid. Yield: 2.13 g (79%). Orange crystals suitable for X-ray diffraction were obtained from a solution of CH_2Cl_2 layered with toluene and pentane at 4 °C. ^{1}H NMR ($CDCl_3$): δ 7.94−5.05 (m, 2H, PPh), 7.31−7.52 (m, 8H, PPh), 7.15−7.24 (m, 1H, H^{12}), 7.07−7.15 (m, 1H, H^{14}), 6.95−7.05 (m, 1H, H^{15}), 6.45−6.55 (m, 1H, H^{13}), 5.66 (d, $^3J_{HH}$ = 6.1, 1H, H^3), 5.42 (d, $^3J_{HH}$ = 4.7, 1H, H^6), 5.10 (d, $^3J_{HH}$ = 6.1, 1H, H^2), 4.74 (d, $^3J_{HH}$ = 5.0, 1H, H^5), 2.60 (sept, $^3J_{HH}$ = 6.8, 1H, H^8), 2.10 (s, 3H, H^7), 1.21 (d, $^3J_{HH}$ = 6.8, 3H, H^9), 1.10 (d, $^3J_{HH}$ = 6.8, 3H, H^{10}). ^{13}C{^{1}H} NMR ($CDCl_3$): δ 177.7 (d, $^2J_{PC}$ = 20, C^{16}), 138.6 (d, $^1J_{PC}$ = 48, PPh_2), 134.9 (d, $^{2/3}J_{PC}$ = 10, PPh_2), 132.5 (d, $^4J_{PC}$ = 2, C^{14}), 131.9 (br, C^{12}), 131.4 (d, $^{2/3}J_{PC}$ = 10, PPh_2), 130.7 (d, $^4J_{PC}$ = 3, PPh_2), 129.9 (d, $^4J_{PC}$ = 3, PPh_2), 129.3 (d, $^1J_{PC}$ = 57, PPh_2), 128.5 (d, $^{3/2}J_{PC}$ = 10, PPh_2), 128.1 (d, $^{3/2}J_{PC}$ = 11, PPh_2), 119.6 (d, $^3J_{PC}$ = 9, C^{15}), 115.1 (d, $^3J_{PC}$ = 7, C^{13}), 113.9 (d, $^1J_{PC}$ = 56, C^{11}), 104.9 (s, C^4), 95.7 (s, C^1), 92.5 (d, $^2J_{PC}$ = 6, C^2), 86.5 (d, $^2J_{PC}$ = 6, C^5), 86.3 (d, $^2J_{PC}$ = 3, C^3), 85.4 (d, $^2J_{PC}$ = 4, C^6), 30.7 (s, C^8), 22.3 (s, C^9 + C^{10}), 18.0 (s, C^7). ^{31}P{^{1}H} NMR ($CDCl_3$): δ 50.5 (s, 1P). Anal. Calcd for $C_{28}H_{28}ClOPRu$ (548.03 g mol^{-1}): C, 61.37; H, 5.15. Found: C, 61.20; H, 5.10.

Preparation of [$Ru(PPh_3)(\eta^2$-PPh_2(*o*-C_6H_4O))(η^6-*p*-cymene)]PF_6 (2). A suspension of [$RuCl(\eta^2$-PPh_2(*o*-C_6H_4O))(η^6-*p*-cymene)] (1.00 g, 1.82 mmol) and PPh_3 (1.30 g, 5.00 mmol) in EtOH (100 mL) was heated at reflux for 2 h. The solution was cooled to RT and a solution of [NH_4]PF_6 (0.81 g, 5.00 mmol) in water (100 mL) added. The solid was then isolated by decantation and washed with water (3 × 50 mL). The solid was then dissolved in CH_2Cl_2 and dried with Na_2SO_4 and the product precipitated by addition of excess diethyl ether. Yield: 0.89 g (53%) as a yellow powder. ^{1}H NMR ($CDCl_3$): δ 6.4−8.0 (m, 25H, PPh), 7.06−7.12 (m, 1H, H^{14}), 7.00−7.06 (m, 1H, H^{12}), 6.82 (dd, $^3J_{PH}$ = 8, $^3J_{HH}$ = 5.3, 1H, H^{15}), 6.48−6.57 (m, 1H, H^{13}), 5.51 (d, $^3J_{HH}$ = 5.9, 1H, H^3), 5.25−5.30 (m, 1H, H^2), 5.09−5.17 (m, 1H, H^6), 4.98 (d, $^3J_{HH}$ = 5.9, 1H, H^5), 2.62 (sept, $^3J_{HH}$ = 6.9, 1H, H^8), 1.90 (s, 3H, H^7), 1.25 (d, $^3J_{HH}$ = 6.9, 3H, H^9), 1.16 (d, $^3J_{HH}$ = 6.8, 3H, H^{10}). ^{13}C{^{1}H} NMR ($CDCl_3$): δ 178.1 (d, $^2J_{PC}$ = 20, C^{16}), 137.7 (d, $^1J_{PC}$ = 51, PPh_2), 133.8 (br, PPh_3), 133.3 (br, C^{12}), 132.8 (d, $^4J_{PC}$ = 1, C^{14}), 132.5 (d, $^{2/3}J_{PC}$ = 10, PPh_2), 131.5 (d, $^{2/3}J_{PC}$ = 10, PPh_2), 131.0 (d, $^4J_{PC}$ = 2, PPh_2), 130.9 (d, $^4J_{PC}$ = 2, PPh_2), 130.8 (br, PPh_3), 129.2 (d, $^{3/2}J_{PC}$ = 11, PPh_2), 128.8 (d, $^{3/2}J_{PC}$ = 11, PPh_2), 128.3 (br, PPh_3),

Table 7. Crystal Data and Details of the Structure Determinations

	1a	1c	1d	5
formula	$C_{36}H_{40}ClF_6P_3Ru$	$C_{49}H_{50}ClF_6P_3Ru\cdot 2CH_2Cl_2$	$C_{43}H_{46}ClF_6P_3Ru\cdot 2CH_2Cl_2$	$2(C_{28}H_{28}ClOPRu)\cdot CHCl_3$
M	816.11	1152.17	1076.08	1215.36
T [K]	100(2)	140(2)	140(2)	140(2)
cryst syst	monoclinic	orthorhombic	orthorhombic	monoclinic
space group	$P2(1)/c$	$Pbca$	$Pna2(1)$	$P2(1)/c$
a [Å]	16.448(3)	16.4780(13)	24.0009(15)	17.4380(12)
b [Å]	10.956(2)	18.9480(14)	11.5170(7)	22.1460(15)
c [Å]	19.134(4)	32.554(3)	16.6737(11)	14.6340(10)
α [deg]				
β [deg]	93.26(3)			103.876(6)
δ [deg]				
V [Å^3]	3442.4(12)	10164.2(14)	4608.9(5)	5486.5(6)
Z	4	8	4	4
density μ [g cm^{-3}]	1.575	1.506	1.551	1.471
μ [mm^{-1}]	0.732	0.723	0.791	0.893
θ range [deg]	$3.10 < \theta < 25.03$	$2.99 < \theta < 25.03$	$3.10 < \theta < 25.03$	$3.01 < \theta < 25.03$
no. of measd reflns	35 341	59 683	27 346	32 203
no. of unique reflns	6012 [$R_{int} = 0.0859$]	8868 [$R_{int} = 0.1077$]	7478 [$R_{int} = 0.0950$]	9584 [$R_{int} = 0.0997$]
no. data/restr/params	6012/36/429	8868/66/638	7478/361/548	9584/578/695
R1, wR2 [$I > 2\sigma(I)$][a]	R1 = 0.0641, wR2 = 0.1258	R1 = 0.0672, wR2 = 0.1497	R1 = 0.0625, wR2 = 0.1282	R1 = 0.0467, wR2 = 0.0565
GoF[b]	1.254	1.079	0.863	0.754[c]

[a] $R1 = \sum||F_o| - |F_c||/\sum|F_o|$, $wR2 = \{\sum[w(F_o^2 - F_c^2)^2]/\sum[w(F_o^2)^2]\}^{1/2}$. [b] $GoF = \{\sum[w(F_o^2 - F_c^2)^2]/(n-p)\}^{1/2}$ where n is the number of data and p is the number of parameters refined. [c] The GoF is lower than normal owing to weak reflections, although the low angle data are good. If reflections with $\theta < 23°$ are taken, the structure converges with a GoF = 0.939 and a completeness of 0.997.

123.1 (t, $^2J_{PC} = 2$, C^4), 120.5 (d, $^3J_{PC} = 10$, H^{15}), 115.9 (d, $^3J_{PC} = 7$, C^{13}), 115.3 (d, $^2J_{PC} = 56$, C^{11}), 99.0 (s, C^1), 97.9 (d, $^2J_{PC} = 3$, C^6), 96.3 (d, $^2J_{PC} = 3$, C^2), 92.8 (d, $^2J_{PC} = 8$, C^3), 86.6 (d, $^2J_{PC} = 9$, C^5), 31.4 (s, C^8), 22.8 (s, C^9), 20.8 (s, C^{10}), 18.1 (s, C^7). $^{31}P\{^1H\}$ NMR ($CDCl_3$): δ 54.3 (d, $^2J_{PP} = 48$, 1P, $RuPPh_2$), 26.0 (d, $^2J_{PP} = 48$, 1P, $RuPPh_3$), −144.2 (sept, $^1J_{PF} = 713$, 1P, PF_6). ESI-MS (CH_2Cl_2) positive ion: m/z 775 $[M]^+$; negative ion: m/z 145 $[PF_6]^-$. Anal. Calcd for $C_{46}H_{43}F_6OP_3Ru$ (919.83 g mol^{-1}): C, 60.07; H, 4.71. Found: C, 60.41; H, 4.80.

Preparation of [$RuCl_2$(P(*p*-tol)$_3$)(η^6-*p*-cymene)]. A solution of [$RuCl_2$(η^6-*p*-cymene)]$_2$ (1.00 g, 1.63 mmol) and P(*p*-tol)$_3$ (1.49 g, 4.85 mmol) in CH_2Cl_2 (50 mL) was stirred at RT for 3 h. The product was precipitated by addition of hexane (120 mL) and concentration of the solution. Recrystallization from CH_2Cl_2−hexane gave the product as an orange powder. Yield: 1.75 g (88%). ^1H NMR ($CDCl_3$): δ 7.10−7.78 (m, 12H, PC_6H_4Me), 5.21 (d, $^3J_{HH} = 5.9$, 2H, H^3), 4.97 (d, $^3J_{HH} = 5.6$, 2H, H^2), 2.90 (sept, $^3J_{HH} = 6.9$, 1H, H^6), 2.36 (s, 9H, PC_6H_4Me), 1.88 (s, 3H, H^5), 1.13 (d, $^3J_{HH} = 6.9$, 6H, H^7). $^{13}C\{^1H\}$ NMR ($CDCl_3$): δ 140.3 (d, $^4J_{PC} = 3$, PC_6H_4Me), 134.3 (d, $^2J_{PC} = 10$, PC_6H_4Me), 130.7 (d, $^1J_{PC} = 48$, PC_6H_4Me), 128.7 (d, $^3J_{PC} = 10$, PC_6H_4Me), 111.1 (d, $^2J_{PC} = 4$, C^4), 95.7 (s, C^1), 88.8 (d, $^2J_{PC} = 3$, C^2), 87.2 (d, $^2J_{PC} = 6$, C^3), 30.3 (s, C^6), 21.9 (s, PC_6H_4Me), 21.4 (s, C^7), 17.8 (s, C^5). $^{31}P\{^1H\}$ NMR ($CDCl_3$): δ 23.0 (s, 1P). Anal. Calcd for $C_{31}H_{35}Cl_2PRu$·(610.57 g mol^{-1})·0.2(CH_2Cl_2): C, 59.71; H, 5.69. Found: C, 60.01; H, 5.50.

Preparation of [RuCl(P(*p*-tol)$_3$)$_2$(η^6-*p*-cymene)]PF_6 (6). A suspension of [$RuCl_2$(P(*p*-tol)$_3$)(η^6-*p*-cymene)] (0.50 g, 0.82 mmol), PPh_3 (0.274 g, 0.90 mmol), and $[NH_4]PF_6$ (0.174 g, 1.07 mmol) in MeOH (30 mL) was stirred at 35 °C for 2 h. The solvent was removed in vacuo and the residue extracted through Celite with CH_2Cl_2 (ca. 40 mL). The product was then isolated by precipitation with hexane (ca. 150 mL) and washed with EtOH (2 × 20 mL) and pentane (1 × 10 mL). Yield: 0.67 g (79%) as a yellow powder. ^1H NMR ($CDCl_3$): δ 6.94−7.38 (m, 24H, PC_6H_4Me), 5.45−5.56 (m, 2H, H^2), 5.06 (d, $^3J_{HH} = 6.2$, 1H, H^3), 2.71 (sept, $^3J_{HH} = 6.9$, 1H, H^6), 2.38 (s, 18H, PC_6H_4Me), 1.24 (d, $^3J_{HH} = 7.0$, 6H, H^7), 1.07 (s, 3H, H^5). $^{13}C\{^1H\}$ NMR ($CDCl_3$): δ 140.6 (s, PC_6H_4Me), 129−134 (m, PC_6H_4Me), 131 (C^4), 100.0 (s, C^1), 97.3 (br, C^2), 88.9 (t, $^2J_{PC} = 5$, C^3), 31.3 (s, C^6), 21.4 (s, C^7), 21.3 (s, PC_6H_4Me), 15.3 (s, C^5). $^{31}P\{^1H\}$ NMR ($CDCl_3$): δ 19.2 (s, 2P), −144.4 (sept, $^1J_{PF} = 713$, 1P, PF_6). Anal. Calcd for $C_{52}H_{56}ClF_6P_3Ru$ (1024.45 g mol^{-1}): C, 60.97; H, 5.51. Found: C, 61.00; H, 5.24.

Kinetics Experiments. Exchange kinetics of **1**−**3** with P(*p*-tol)$_3$ were monitored using $^{31}P\{^1H\}$ NMR spectroscopy, integrating relative to an internal standard of $PO(OEt)_3$ in toluene (in sealed capillary tubes). Ru concentrations were ∼5 mM. Equilibration of **1c** was monitored using $^{31}P\{^1H\}$ NMR spectroscopy in THF. Ru concentrations were ∼20 mM. All samples were prepared under nitrogen and then transferred into screw-cap NMR tubes under nitrogen. The temperature was determined before and after each measurement using an external temperature probe and showed good agreement (±0.2 K). Integrations were preformed using NMRICMA, an iterative fitting application for MatLab.[24]

All exchange reactions of **1**−**3** showed excellent first-order behavior under the conditions (full data are listed in Table S2). Data for the reactions involving only one ligand exchange (20 equiv of P(*p*-tol)$_3$/Ru) were fitted to single-exponential functions (Origin 7.0). Treatment of data for complexes with sequential exchange reactions (30 equiv of P(*p*-tol)$_3$/Ru) was carried out by least-squares fitting of eqs 1−3 with Scientist 2.0 (example fit is given in Figure 5 and corresponds to entries 2 and 6 in Table S2).[25] The multistep treatment for complex **1d** is only necessary at one temperature owing to large difference in rates of exchange; single-exponential functions are used for all other temperatures.

$$[A] = e^{-k_1(t-t_1)}[A]_0 \quad (1)$$

$$[B] = \frac{k_1[A]_0(e^{-k_2(t-t_1)} - e^{-k_1(t-t_1)})}{k_2 - k_1} \quad (2)$$

$$[C] = [A]_0\left(1 + \frac{k_1 e^{-k_2(t-t_1)} - k_2 e^{-k_1(t-t_1)}}{k_2 - k_1}\right) \quad (3)$$

The rate constants for the forward (k_3) and reverse reactions (k_{-3}) were calculated from the rate of approach to equilibrium (eq 4) and the equilibrium constant ($k_{-3} = k_3K^{-1}$).[26] The activation parameters for the forward and reverse reactions were determined

(24) Helm, L.; Borel, A.; Yerly, F. *NMRICMA* 3.0 for Matlab; Institut des Sciences et Ingénierie Chimiques: EPFL Lausanne, 2004.

from the temperature dependence of the rate constants using the Eyring equation. Full data are found in Table S3.

$$[1c] = \frac{[1c]_0(1 + e^{-8k_3t})}{2} \quad (4)$$

Catalytic Evaluations. All catalytic experiments were conducted using a home-built multicell autoclave containing an internal temperature probe. Each glass reaction vessel was charged with the precatalyst (5.0×10^{-6} mol), styrene (0.01 mol, S:C = 2000: 1, ACROS, dried over molecular sieves), internal standard (100 mg octane, distilled from CaH_2 under nitrogen and stored under nitrogen over molecular sieves), and solvent (2 mL of THF, dried catalytically under nitrogen and stored under nitrogen over molecular sieves) and then placed inside the autoclave, which was then flushed with H_2 (3×10 bar). The autoclave was then heated to the desired temperature under H_2 (5 bar) and then maintained at 50 bar for the duration of the catalytic run (60 min). The autoclave was then cooled to ambient temperature using an external water-cooling jacket and the pressure released. Conversions were determined by GC analysis of the samples using a Varian Chrompack CP-3380 gas chromatograph. Ethyl benzene was the only product observed.

Crystallography. Relevant details about the structure refinements are given in Table 7, and selected geometrical parameters for **1a**, **1c** and **1d** are found in Table 2. Data were collected on a KUMA CCD diffractometer system (**1c**, **1d**, **5**) and Bruker APEX II CCD diffractometer system (**1a**) using graphite-monochromated Mo Kα radiation (0.71073 Å) and a low-tempetature device. Data reduction was performed using CrysAlis RED[27] (**1c**, **1d**, **5**) and EvalCCD[28,29] (**1a**). Structures were solved using SIR97[30] and refined (full-matrix least-squares on F^2) using SHELXTL.[28,31] Absorption corrections were applied to the data sets of **1a** (multiscan, SADABS),[28] **1c** (empirical, DELABS),[32] and **1d** (empirical multiscan).[33] The structure of **1d** was refined using the twinned refinement method, with a BASF parameter of 0.09056. All non-hydrogen atoms were refined anisotropically, with hydrogen atoms placed in calculated positions using the riding model with the exception of those on C8 in **5**, which were located on the Fourier difference map and then constrained. Disorder in the counterion in **1c** was modeled by splitting it over two sites. Disorder in the *p*-cymene ring of one of conformations in the asymmetric cell of **5** was modeled by splitting the isopropyl moiety over two sites. Disorder in the phenyl rings of the other conformation of **5** was modeled by splitting them over two sites, restraining the geometry of the rings and restraining the displacement parameters. Restraints were also applied to the displacement parameters of other atoms in these two conformations of **5**, the coordinated atoms of the *p*-cymene ring in **1a**, selected atoms of the counterion and solvent in **1c**, and to all atoms in the structure of **1d**. Graphical representations of the structures were made with ORTEP3.[34]

Acknowledgment. This work was supported by the EPFL and the Swiss National Science Foundation. We are grateful to Dr. R. Scopelliti and Dr. E. Solari for assistance with crystallography and Dr. G. Laurenczy for helpful discussions. We also thank the New Zealand Foundation for Research, Science and Technology for a Top Achiever Doctoral Fellowship (A.B.C.).

Supporting Information Available: Crystallographic information for **1a**, **1c**, **1d**, and **5** in CIF format and Tables S1−S3. This material is available free of charge via the Internet at http://pubs.acs.org.

OM070050D

(25) The system is under pseudo-first-order conditions, and the reactions are considered irreversible owing to the large excess of P(*p*-tol)$_3$ (Scheme 3). The concentrations of the initial complex A, intermediate B, and final complex C were the dependent variables and *t* the independent. The parameters t_1, k_1, k_2, and $[A]_0$ ([A], [B], [C] were in arbitrary units) were refined during the fitting.

(26) Moore, J. W.; Pearson, R. G. *Kinetics and Mechanism*, 3rd ed.; John Wiley & Sons: New York, 1981; p 304.

(27) *CrysAlis RED*; Oxford Diffraction Ltd.: Abingdon, Oxfordshire, U.K., 2003.

(28) *EvalCCD*; Bruker AXS, Inc.: Madison, WI, 1997.

(29) Duisenberg, A. J. M.; Kroon-Batenburg, L. M. J.; Schreurs, A. M. M. *J. Appl. Crystallogr.* **2003**, *36*, 220.

(30) Altomare, A.; Burla, M. C.; Camalli, M.; Cascarano, G. L.; Giacovazzo, C.; Guagliardi, A.; Moliterni, A. G.; Polidori, G. G.; Spagna, R. *J. Appl. Crystallogr.* **1999**, *32*, 115.

(31) Sheldrick, G. M. *SHELXTL*; University of Göttingen: Germany, 1997.

(32) Walker, N.; Stuart, D. *Acta Crystallogr. Sect. A* **1983**, *39*, 158.

(33) Blessing, R. H. *Acta Crystallogr.* **1995**, *A51*, 33.

(34) Farrugia, L. J. *J. Appl. Crystallogr.* **1997**, *30*, 565.